GALACTIC MAGNETIC FIELDS, COSMIC RAYS AND WINDS
Part 2

Michał Hanasz

Centre for Astronomy, Nicolaus Copernicus University, Toruń, Poland

II Cosmology School, Kielce, 18.07.2016

Synchrotron emissivity from cosmic-ray electrons with a power-law energy spectrum in a volume with a magnetic field strength $B_\perp$:

$$\varepsilon \sim N_0 \nu^{(\gamma+1)/2} B_\perp^{(1-\gamma)/2},$$

where ν is the frequency, ε is the density of CR electrons per energy interval, γ is the spectral index of the power-low energy spectrum of CR electrons ($\gamma = -2.8$ in the ISM).
The intrinsic degree of linear polarisation of synchrotron emission

$$p_0 = \frac{1-\gamma}{7/3-\gamma}$$

For $\gamma = -2.8$ maximum polarisation degree is $p_0 = 74\%$,
E-vector is normal to magnetic field direction.

Faraday rotation

The rotation angle Φ of wave polarisation plane, due to different phase speeds of right– and left–circular polarisation components of radio waves

$$\Phi = k\lambda^2 \int n_e B_{||} \, dl,$$

where λ – radio wavelength, n_e – thermal electron density, $B_{||}$ m.f. along the line of sight, path length interval along the line of sight.

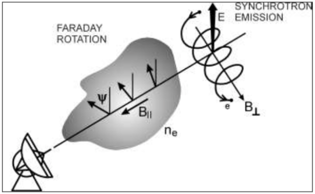

From Beck & Wielbinski (2013)

Regular magnetic field – synchrotron polarisation **and** Faraday rotation.
Turbulent isotropic field – no polarisation, **no** Faraday rotation.
Turbulent anisotropic field (e.g. shock-compressed) – polarisation **and** Faraday rotation.
⇒ **possibility to detect regular (coherent, large-scale) magnetic fields in astrophysical objects.**

M51

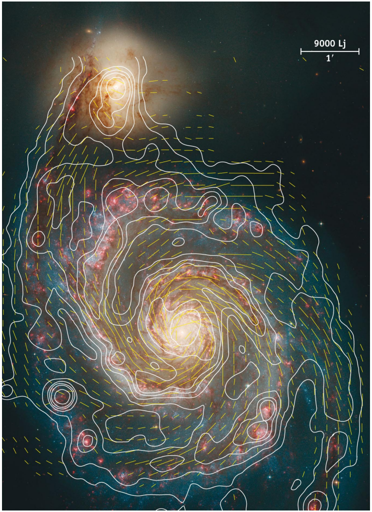

A. Fletcher et al. 2008

NGC891

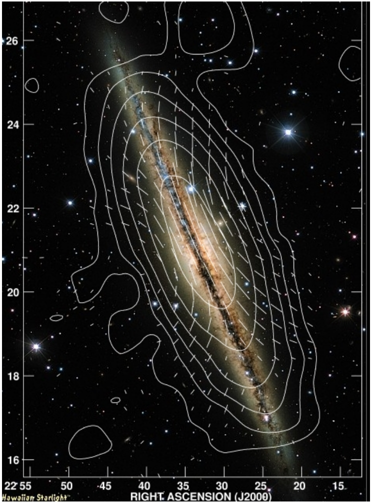

M. Krause et al. 2008

Key observational properties:

- Faraday rotation measurements indicate regular magnetic fields on kpc-scale in galactic magnetic fields
- Approximate equipartition of magnetic fields, gas turbulent motion and cosmic rays
- Horizontally aligned, spiral magnetic fields, pitch angles in the range of 10-30 deg
- X-shaped m.f structures observed in edge-on galaxies
- Magnetic arms (regular magnetic field) in between optical arms in some cases (e.g.. NGC6946)
- comparable magnitudes of the turbulent and regular magnetic field components.
- μG magnetic fields observed on all kinds of disk galaxies, up to $z = 3$, indicating that magnetic field amplification processes have to be very efficient.
- The FIR-RADIO correlation strongly indicates a tight relation between magnetic field generation and star formation in galaxies $L_{1.4GHz} \propto \mathrm{SFR}^{1.25}$

- Two types of dynamo are considered in the context of galactic and extragalactic magnetic fields:
  - → **large-scale (mean field) dynamos:** amplification of magnetic fields coherent on length-scales much larger than the scales of the energy-carrying turbulent eddies.
  - → **small-scale (fluctuation) dynamos:** fast amplification of magnetic fields on length-scales smaller than the scales of energy carrying eddies.

Direct simulation of SN driven dynamo
Gressel et al. 2008a, 2008b

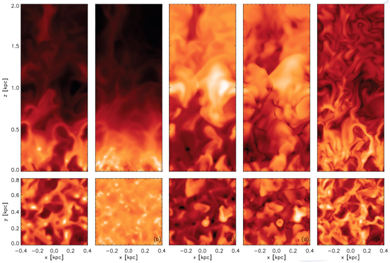

Displayed quantities: number density, column density, temperature, velocity dispersion, mag. fileld strength

- 3D local patch of interstellar medium
- vertical stratification up to ±6 kpc
- sheared galactic rotation
- localised thermal energy input – supernovae
- optically thin radiative
- heating/cooling

Gressel et al. 2008a, 2008b (cont.)

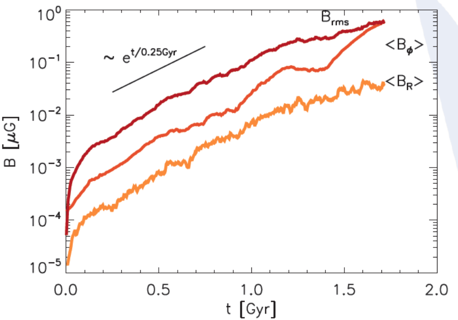

- Exponential amplification of the regular magnetic field, although the galactic rotation angular velocity enlarged artificially ($\sim$ 2x)
- high pitch angles up to 35^o
- **Results consistent with the mean-field dynamo theory**

Wang & Abel 2009 (see also Beck A. et al 2012, Sur et al 2012)

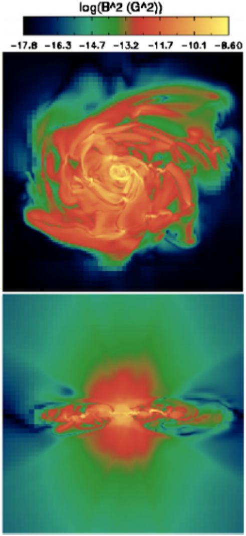

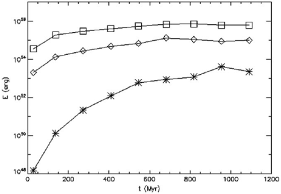

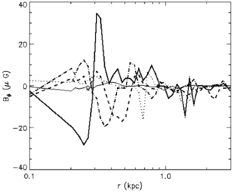

- Amplification a seed field of 10^{-9} G to μG level in $\sim$ 500 Myr. The e-folding time of magnetic energy before saturation is $\sim$ 50 Myr.
- After saturation, the toroidal field in the disk dominates over the vertical component, while in the magnetised halo, the vertical component dominates over the toroidal component.

Kotarba et al 2011, MNRAS 415, 3189

- **SPH/N-body simulations of galaxy collisions**
- radiative cooling, star formation, SN feedback
- initial MF - disk: $(10^{-9} - 10^{-6}\mu G)$, IGM: $(10^{-9} - 10^{-6}\mu G)$
- **Magnetic field strength grows in galactic disks and in the IGM**
- **magnetic field saturation at $1\mu G$ within the galaxies and $10^{-2}\mu G$ in the IGM independent of the initial value**

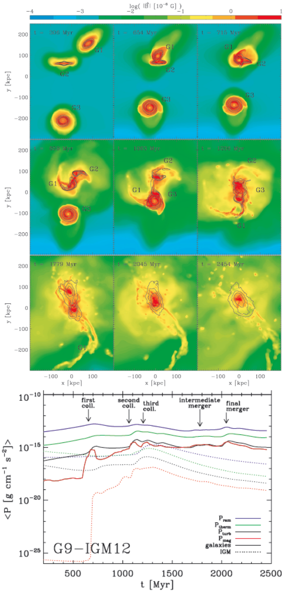

Parker instability in the ISM (Parker 1966, 1967)

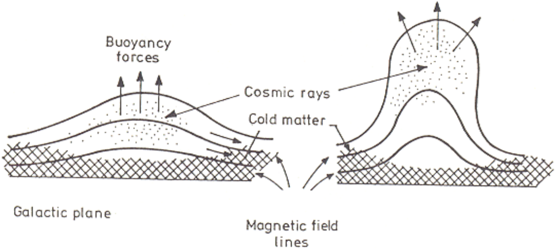

(from *High Energy Astrophysics, M. Longair, 2011, p. 522)*

- Cosmic ray gas: an important ISM ingredient - accelerated in SN remnants (see e.g. Hillas 2005, Ackermann et al. 2013)
- Kinetic energy of SN II explosion $\sim 10^{51}$erg $\Rightarrow$ 10 % of $E_{\rm SN}$ $\rightarrow$ acceleration of cosmic rays - charged particles (protons, electrons) accelerated in shocks to relativistic energies
- $\Rightarrow$ strong buoyancy effects of the relativistic weightless CR gas.

MHD EQUATIONS

$$\frac{\partial \boldsymbol{V}}{\partial t} + (\boldsymbol{V} \cdot \nabla)\boldsymbol{V} = -\frac{1}{\rho}\nabla(p + p_{CR}) + \boldsymbol{g} + \frac{1}{\rho}\nabla\left(\frac{B^2}{8\pi}\right) + \frac{\boldsymbol{B} \cdot \nabla \boldsymbol{B}}{4\pi\rho}$$

$$\frac{\partial \rho}{\partial t} + \nabla \cdot (\rho \boldsymbol{V}) = 0$$

$$p = c_s^2 \rho \qquad \text{(isoth.approx)}$$

$$\frac{\partial \boldsymbol{B}}{\partial t} = \nabla \times (\boldsymbol{V} \times \boldsymbol{B}) + \eta \nabla^2 B$$

CR TRANSPORT EQUATION

Diffusion - advection approximation

(e.g. Schlickeiser & Lerche 1985, A&A, 151, 151)

$$\frac{\partial e_{\rm cr}}{\partial t} + \nabla(e_{\rm cr}\boldsymbol{V}) = -p_{\rm cr}\nabla\boldsymbol{V} + \nabla(\hat{K}\nabla e_{\rm cr}) \quad (1)$$

$$+ \text{CR sources (SN remnants)}$$

$$p_{\rm cr} = (\gamma_{\rm cr} - 1)e_{\rm cr} \quad (2)$$

Anisotropic diffusion of CRs

(Giaccalone & Jokipii 1998 , Jokipii 1999, Ryu et al. 2003)

$$K_{ij} = K_{\perp}\delta_{ij} + (K_{\parallel} - K_{\perp})n_i n_j, \quad n_i = B_i/B, \quad (3)$$

$$K_{\parallel} = 3\cdot 10^{28}\text{cm}^{2}\text{s}^{-1}, \qquad K_{\perp} = (1-10)\%\,(K_{\parallel})$$

GALACTIC DISK MODEL – MILKY WAY TYPE GALAXY

(Hanasz et al 2009, ApJ 706L, 155)

- Galactic gravitational potential: halo+bulge+disk: analytical model (Allen & Santillan 1991), N-body model (Hernquist 1993)
- Interstellar gas: Global model of ISM for the Milky Way (Ferriere 1998)
- **Schmidt-Kennicutt law:** SFR $\propto$ (gas density)$^{1.4}$
- SNR $\propto$ SFR
- 10% of of SN energy output is converted to CR energy.
- **No magnetic field at** $t = 0$
- **weak** ($10^{-4}\mu$**G) dipolar, small scale (**$r \sim 50$**pc) randomly oriented magnetic field is supplied locally in 10% of SN remnants (Krab type)**

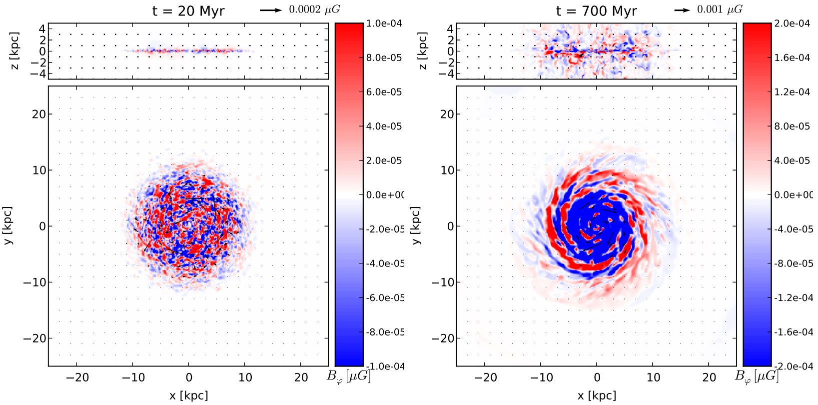

Colours: – azimuthal (toroidal) magnetic field blue: $B_\varphi < 0$, red: $B_\varphi > 0$

Exploding magnetised stars spread weak irregular magnetic fields in the ISM

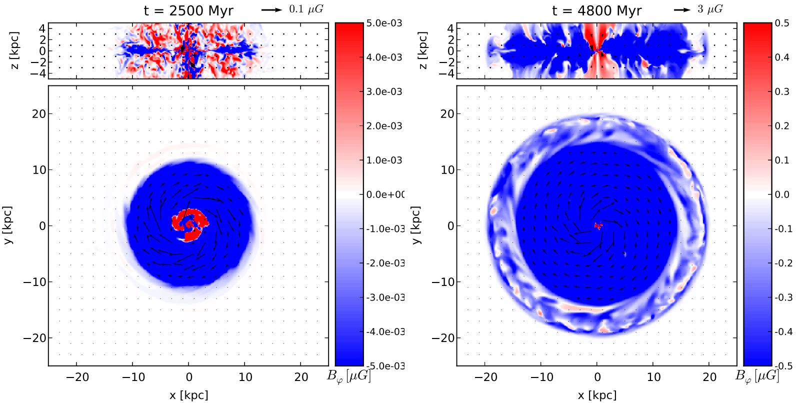

Colours: – azimuthal (toroidal) magnetic field blue: $B_\varphi < 0$, red: $B_\varphi > 0$

- Cosmic-ray driven **buoyancy, Coriolis force and disk differential rotation** lead to amplification (timescale $\sim T_{rot}$) of magnetic field – $\alpha\omega$-type dynamo.
- **Galactic wind** evacuates selectively one of magnetic polarities $\Rightarrow$ regularisation of magnetic field.

GROWTH OF MAGNETIC FLUX AND ENERGY IN THE GLOBAL DISK

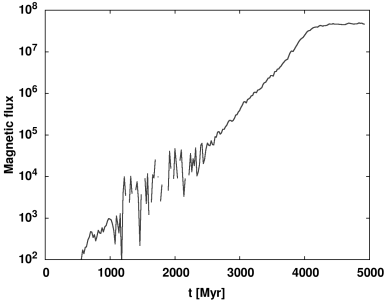

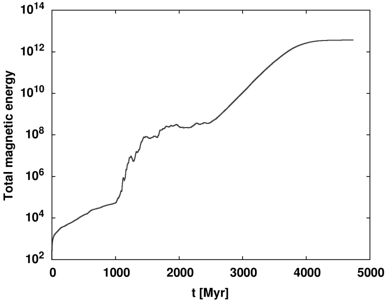

Amplification timescale of the large-scale magnetic field:

$$T_{\langle B \rangle} = 270\text{Myr} \simeq T_{rot}$$

Parker instability + magnetic reconnection

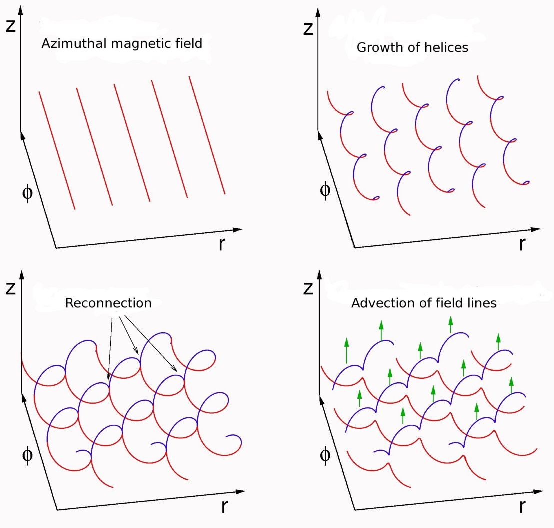

Hanasz & Lesch (1998)

Gravitational potential from N-body simulations – VINE (Wetzstein et al 2008), MHD+CR – PIERNIK

Dominik Wóltański PhD thesis (2015)

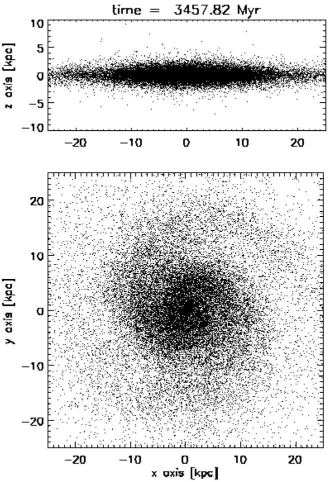

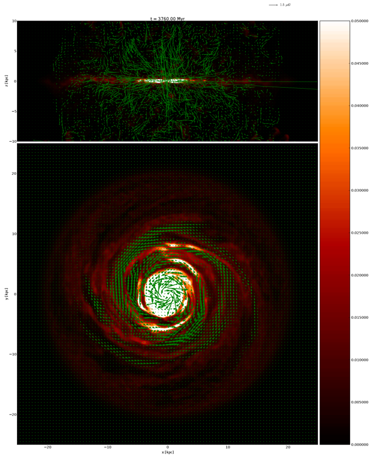

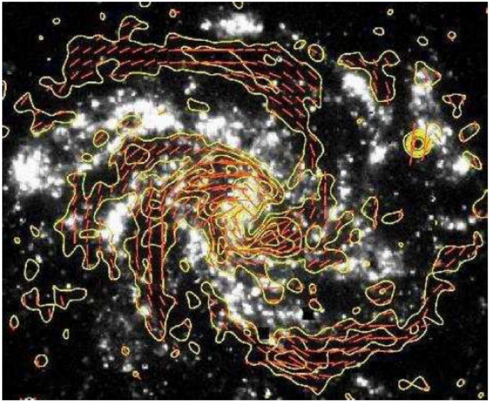

MAGNETIC ARMS IN BETWEEN OPTICAL ARMS OF NGC6946

(Beck & Hoernes 1996, Beck 2011)

EFFECT PREDICTED BY OUR MODEL !

HELICAL MAGNETIC FIELD IN HALO

3D volume rendering of azimuthal magnetic field component, rotation of the viewpoint, fixed time.

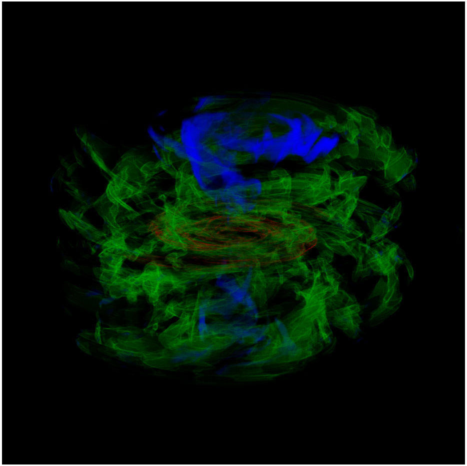

Galactic wind drags the regular magnetic field from the disc

$\Rightarrow$ MAGNETIC HELICES

MAGNETIC FIELD STRUCTURE RESULTING AS PROJECTION OF THE WIND-SHAPED HELICES

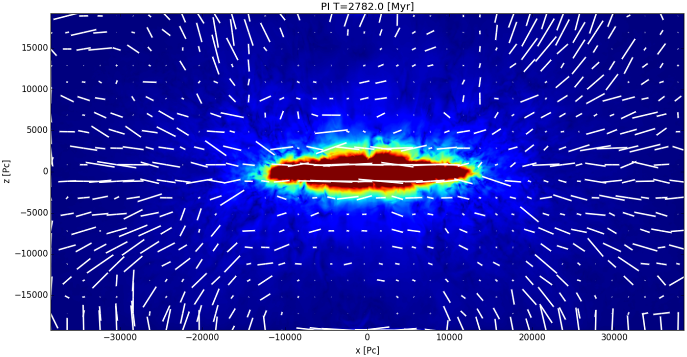

Colour: polarised synchrotron intensity integrated along the line of sight
Vectors: polarisation vectors of synchrotron emission
(direction $\parallel \vec{B}$, length $\propto$ polarisation degree)

X-SHAPED STRUCTURES IN EDGE-ON GALAXIES – EXAMPLES

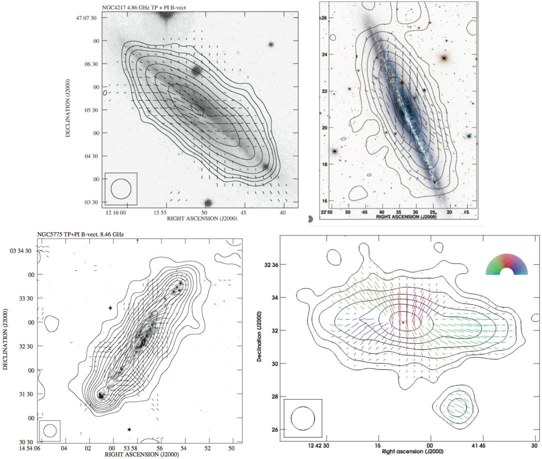

Soida (2005), Krause (2009), Soida (2011), Mora&Krause(2013)

EFFECT PREDICTED BY OUR MODEL !

Large-scale galactic winds are observed in galaxies:
M82 (HST) – classical example of a starburst galaxy.
Wind apparent in H_α emission.

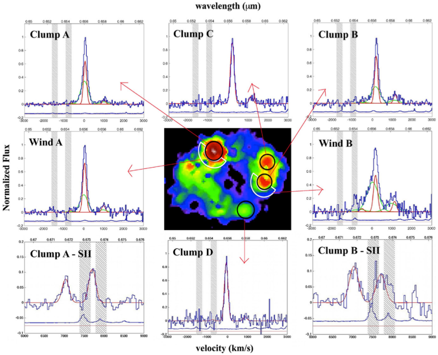

- Galaxies at redshift $z \sim 1.5 - 3$ (e.g. ZC406690, $z \simeq 2$) show powerful galactic winds $v_z \geq 1000\text{km s}^{-1}$ which transport gas away from the galaxy, (e.g.. Genzel et al 2011, Newman et al, ApJ 752, 111, 2012)
- Winds are launched directly from the sites of strongly clustered star formation.

The question of wind origin:

- Type II supernovae – energetic enough to expel gas from galactic disks (Larson 1974)
- However, the thermal energy of SN explosion is mainly deposited at the sites of star formation, i.e. dense molecular clouds.
- **The cooling times are very short** and the energy can be efficiently radiated away making it **difficult to drive large scale galactic winds** (see e.g. Brook et al. MNRAS 415, 1051, 2011; Dalla Vecchia & Shay MNRAS, 426, 140,2012)

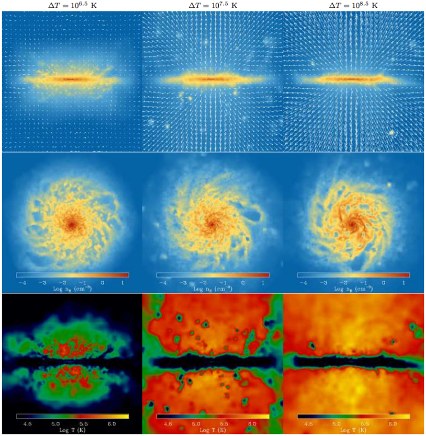

Winds are inefficient if too much gas is heated to too low temperatures with too low cooling times (Dalla Vecchia & Schaye 2012)

- In current ΛCDM cosmological models galaxies form through the cooling of gas at the centers of DM haloes ⇒ star formation (SF).
- Feedback from massive stars has to be considered (White & Rees 1978) – to prevent gas from excessive cooling.
- In absence of stellar feedback all available gas would collapse to stars too quickly — the timescale of gravitational instability is only a few 10 Myr in typical conditions of ISM (see e.g. the review paper by MacLow & Klessen 2004)

Two variants of galaxy formation (same initial conditions)
(Uebler, Naab etal 2014, arXiv 1403.6124)

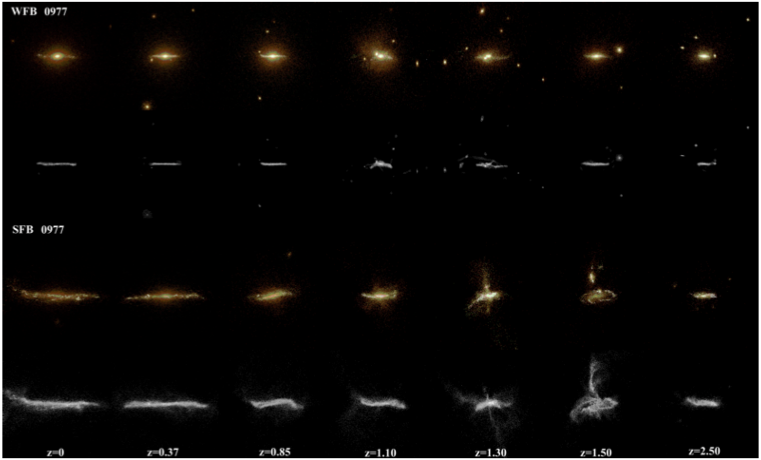

1. weak feedback (WFB) – formation of a bulge-dominated galaxy
2. strong feedback (SFB) – formation of a disk-dominated galaxy

- Numerical simulations show that winds corresponding to strong feedback promote formation of disk-dominated galaxies, while weak feedback leads to formation of bulge-dominated galaxies.
- Winds remove preferentially the low-angular-momentum material from the system: low angular momentum $\rightarrow$ stronger gas condensation $\rightarrow$ stronger star formation $\rightarrow$ stronger winds
- The remaining high-specific-angular-momentum gas forms disks.

Important note:
The strong feedback scenario relies on the *momentum feedback algorithm* – a numerical trick to transport the vertical momentum of SNR expansion from dense gas in the disk to the diluted gas above the disk. A physical mechanism to justify or avoid such a trick is needed.

Cosmic rays can drive strong outflows from gas-rich high-redshift disk galaxies.

Hanasz, Lesch, Naab, Gawryszczak, Kowalik, Wóltański, ApJL, 777, L38 2013

- A galaxy similar to Milky Way (same masses of galactic halo, and stellar disk), but $\sim 10\times$ higher gas contents ($z = 2$).
- **Isothermal gas, no momentum feedback.**
- Fresh gas supplied at the fixed rate $\dot{M}_{in} = 100\,\mathrm{M}_{\odot}/\mathrm{yr}$.
- Toroidal magnetic field, $B_0 = 3\mu$G already present in the disk.
- Self-gravity forms dens gas blobs as soon as gaseous disk becomes gravitationally unstable.

- Star formation rate

$$\dot{\rho}_{\rm SFR} \simeq \epsilon_{ff} \frac{\rho}{\tau_{ff}} \simeq \epsilon_{ff} \sqrt{\frac{G\rho^3}{32\pi}} \propto \rho^{3/2} \quad \text{if} \quad \rho > \rho_{\rm crit}$$

$\tau_{ff} = \sqrt{\frac{32\pi}{G\rho}}$, $\rho_{crit} = 600\text{cm}^{-3}$, $\epsilon_{ff} = 0.1$ — star formation efficiency,

- Massive stars explode as Supernovae, 1SN appears for 100 $M_\odot$ of gas converted to stars.
- Cosmic ray energy density input – 10% of E_{SN}, $E_{SN} \simeq 10^{51}$erg:

$$\Delta e_{CR} = 0.1 E_{SN}\, \dot{\rho}_{\rm SFR}\, \Delta t$$

added to a cell if $\rho > \rho_{\rm crit}$.

- Simulation box $(100\text{kpc})^3$, fixed grid 512^3.

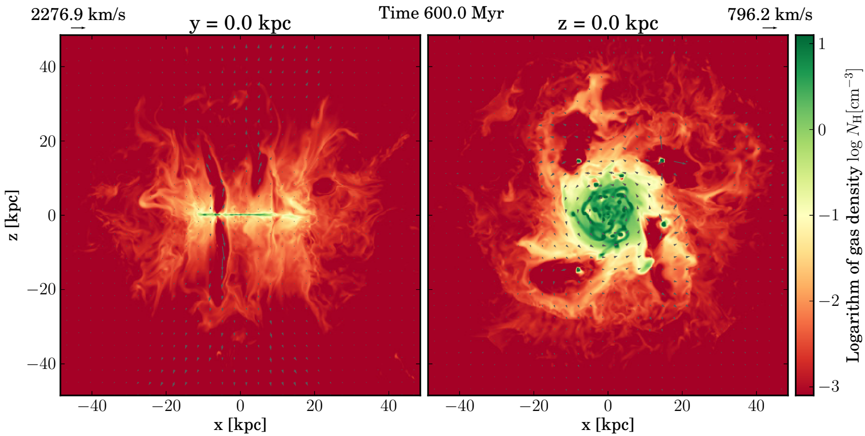

Logarithm of gas density and velocity vectors. Dense gas blobs hosting star formation regions are apparent at the horizontal slice.
Vertical streams of high velocity rarefied gas extend from star forming regions to $z = \pm 20 - 30$kpc

CR ENERGY DENSITY AND MAGNETIC FIELD

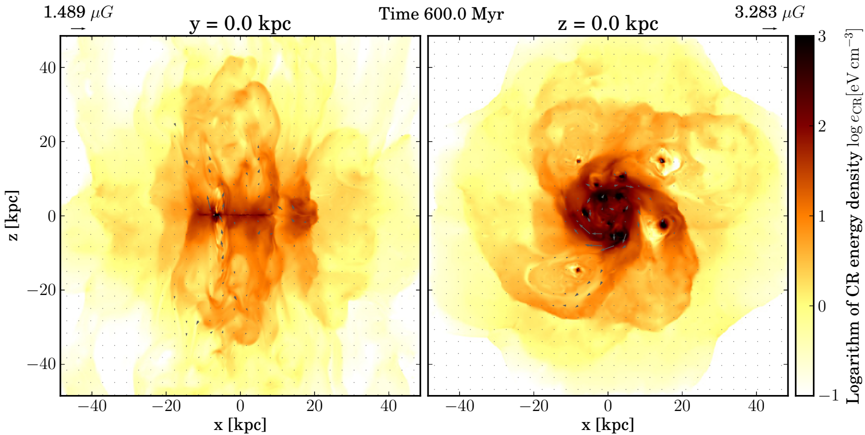

Logarithm of CR energy density and magnetic vectors. The high concentration of CRs at the horizontal plane coincides with the star forming clouds.

VERTICAL VELOCITY

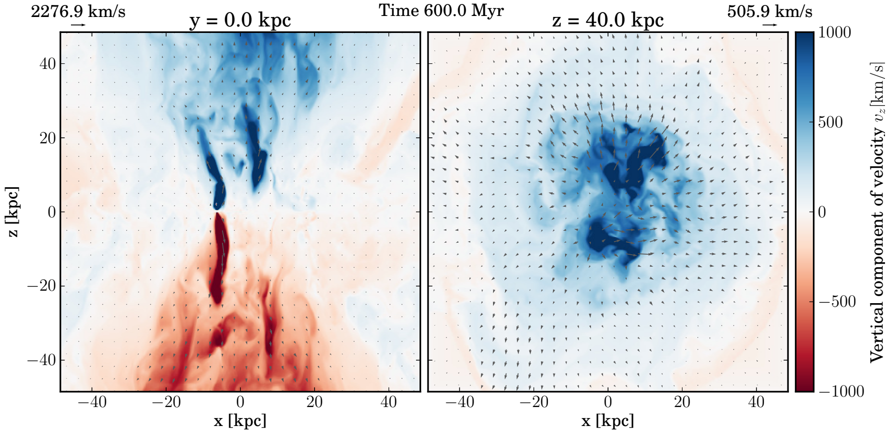

Vertical component of velocity. Collimated streams of high velocity gas extend several 10 kpc above and below the disk.

VERTICAL MAGNETIC FIELD

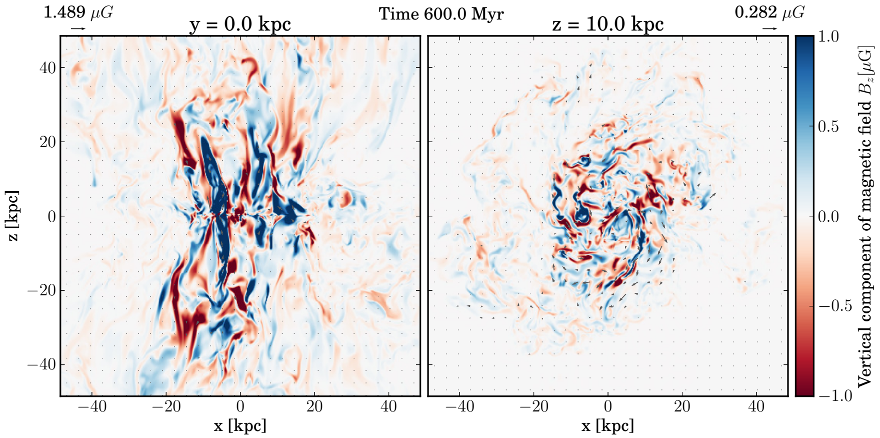

Magnitude of magnetic field **B**. Vertical filaments of $\sim 1\mu$G magnetic field extend to vertical distances of several tens of kpc from the galactic plane.

HORIZONTALLY INTEGRATED MASS FLUX

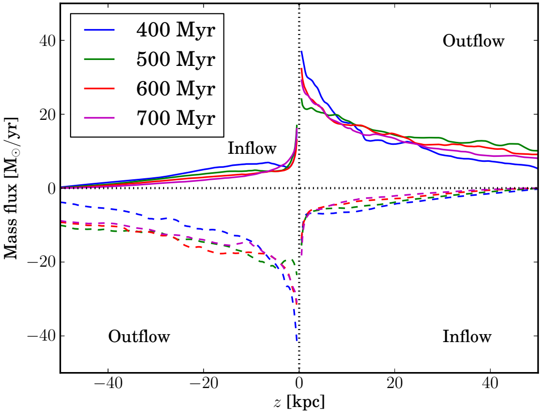

Horizontally integrated mass flux vs. vertical coordinate z. Solid lines denote gas moving in positive z-direction, dashed lines – gas moving in negative z-direction.

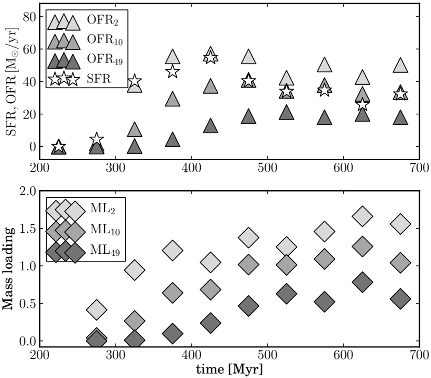

Top: Star formation rate and total mass outflow rate at three different levels $z = \pm 2$kpc , ± 10kpc , and $z = \pm 49$kpc .
Bottom: Mass loading factors ~ 1.

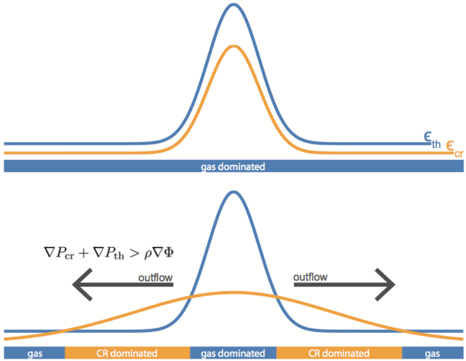

Due to the diffusive nature of CRs the strongest vertical acceleration of gas takes place above and below the dense star forming clouds. Figure taken from Salem and Bryan (2014).
The mechanism is proposed to replace the "momentum feedback" trick.

Salem, Brian, Hymmels, ApJ 797, L18,204

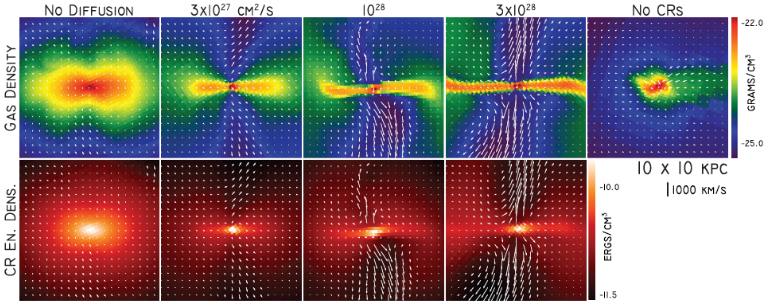

Figure 4. Top: edge-on cutaways of physical gas density with velocity vectors overplotted across our five runs. Diffusive CR runs feature bipolar bulk flows of material away from the central disk. Bottom: the same cutaways, but showing CR energy density.
(A color version of this figure is available in the online journal.)

Recent results confirm the expected effect of selective removal of low-angular-momentum material and formation of flattened disks for the canonical CR diffusivity $K = 2 \times 10^{28}\mathrm{cm}\ ^{2}\mathrm{s}^{-2}$

- 10% of SN energy converted to Cosmic Rays is sufficient to drive large-scale galactic wind in star forming high-redshift galaxies.
- The CR pressure gradient can drive strong bi-polar galactic wind with velocities exceeding 10^3km s^{-1} with mass loading ~ 1 (galactic mass-loss rate comparable to star formation rate).
- Efficient CR-driven wind acceleration is possible because:
  1. CR pressure gradient acts on diluted medium far away from dense gas clouds – due to diffusive nature of CRs.
  2. CRs cool down inefficiently, contrary to shock-heated ISM gas.
- Our results are consistent with the results of similar studies of Booth, et al (2013) and Salem & Bryan (2014).

The Astrophysical Journal Letters, 816:L19 (6pp), 2016 January 10
doi:10.3847/2041-8205/816/2/L19

LAUNCHING COSMIC-RAY-DRIVEN OUTFLOWS FROM THE MAGNETIZED INTERSTELLAR MEDIUM

Philipp Girichidis[1], Thorsten Naab[1], Stefanie Walch[2], Michał Hanasz[3], Mordecai-Mark Mac Low[4,5], Jeremiah P. Ostriker[6], Andrea Gatto[1], Thomas Peters[1], Richard Wünsch[7], Simon C. O. Glover[5], Ralf S. Klessen[5], Paul C. Clark[8], and Christian Baczynski[5]

- Supernova (SN)-driven interstellar medium (ISM) in a stratified box (a small part of galactic disk at high spatial resolution) that dynamically couples the injection and evolution of cosmic rays (CRs) and a self-consistent evolution of the chemical composition.
- The thermodynamic evolution of the gas is computed using a chemical network that follows the abundances of H+, H, H2, CO, C+, and free electrons and includes (self-)shielding of the gas and dust.
- Radiative cooling of inerstellar gas as well as heating of ISM by SN shocks and interstellar radiation feld taken into account.

3 simulations

(in 3 columns)

1. Only thermal SN output $E_{SN} = 10^{51}$erg, no CR
2. Only CR output $10\% E_{SN}$
3. Thermal E_{SN}, CR $10\% E_{SN}$

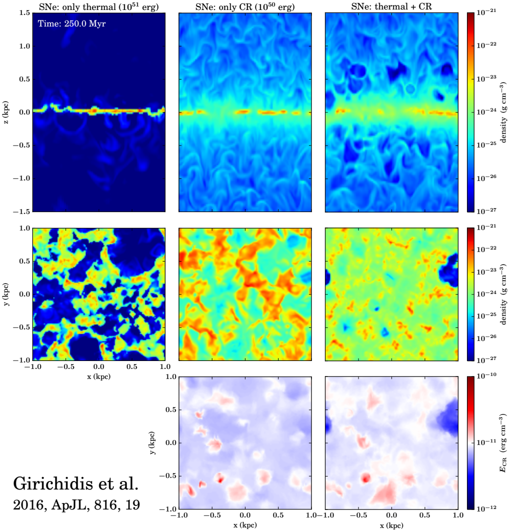

Girichidis et al.
2016, ApJL, 816, 19

Comparison of vertical profiles of the total gas density fo all simulations.

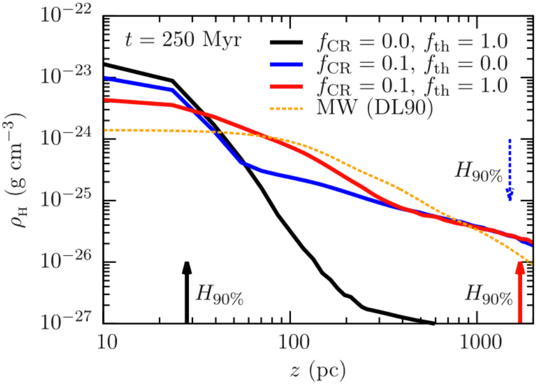

Arrows indicate the height of 90 % of enclosed mass. Yellow dotted line - observed density profile for the MW (Dickey & Lockman 1990).

CR feedback results in extended gas distribution, which is much closer to the observed extent of the gas.

Main conclusions from this work:

- CRs perceptibly thicken the disk with the heights of 90% enclosed mass reaching 1.5 kpc.
- The simulations indicate that CRs alone can launch and sustain strong outflows of atomic and ionized gas with mass loading factors of order unity, even in solar neighborhood conditions and with a CR energy injection per SN of 10^{50}erg, 10% of the thermal energy of a SN.
- The CR-driven outflows have moderate launching velocities close to the midplane (100km s^{-1}) and denser ($\rho \sim 10^{-24} - 10^{-26}$gcm $^{-3}$), smoother, and colder than the purely thermal SN-driven winds.
- The simulations support the importance of CRs for setting the vertical structure of the disk as well as the driving of winds.